Mon. Not. R. Astron. Soc. **377,** 1737–1746 (2007) doi:10.1111/j.1365-2966.2007.11742.x

CCD *BVI* photometry and Coravel observations of stars in the open cluster NGC 2489

Andrés E. Piatti,[1⋆] Juan J. Clariá,[2⋆] Jean-Claude Mermilliod,[3⋆] María C. Parisi[2⋆] and Andrea V. Ahumada[2⋆]

[1]*Instituto de Astronomía y Física del Espacio, CC 67, Suc. 28, 1428 Ciudad de Buenos Aires, Argentina*
[2]*Observatorio Astronómico, Universidad Nacional de Córdoba, Laprida 854, 5000 Córdoba, Argentina*
[3]*Laboratoire d'Astrophysique de l'École polytechnique fédérale de Lausanne, Observatoire, 1290 Sauverny, Switzerland*

Accepted 2007 March 14. Received 2007 March 14; in original form 2007 January 18

ABSTRACT

We present CCD *BVI* photometry for the southern open cluster NGC 2489 and its surrounding field. The sample consists of 2182 stars measured in an area of 13.6×13.6 arcmin^2, extending down to $V \sim 21.5$. These data are supplemented with CORAVEL radial-velocity observations for seven red giant candidates. A cluster angular radius of 6.7 ± 0.6 arcmin, equivalent to 3.5 ± 0.3 pc, is estimated from star counts carried out inside and outside the cluster region. The comparison of the cluster colour–magnitude diagrams with isochrones of the Padova group yields $E(B-V) = 0.30 \pm 0.05$, $E(V-I) = 0.40 \pm 0.05$ and $V - M_V = 12.20 \pm 0.25$ for $\log t = 8.70$ ($t = 500^{+130}_{-100}$ Myr) and $Z = 0.019$. NGC 2489 is then located at 1.8 ± 0.3 kpc from the Sun and 25 pc below the Galactic plane. The analysis of the kinematical data allowed us to confirm cluster membership for six red giants, one of them being a spectroscopic binary. A mean radial velocity of 38.13 ± 0.33 km s^{-1} was derived for the cluster red giants. The properties of a sample of open clusters aligned along the line of sight of NGC 2489 are examined.

Key words: techniques: photometric – stars: kinematics – open clusters and associations: general – open clusters and associations: individual: NGC 2489.

1 INTRODUCTION

The CCD *BVI* photometric data reported in this study were obtained as part of a project that is still being developed at the Observatorio Astronómico de la Universidad Nacional de Córdoba (Argentina). This project aims either at determining the fundamental parameters or at refining the quality of observationally determined properties for some unstudied or poorly studied open clusters in order to improve our understanding of the clusters themselves and the Galaxy as a whole. In some cases, *BVI* photometry proved to be a valuable tool for obtaining the fundamental parameters of star clusters, since information on cluster membership, distance, reddening and age is obtained through the analysis of (V, $B-V$) and (V, $V-I$) colour–magnitude diagrams (CMDs; see e.g. Piatti, Clariá & Ahumada 2006a,b). In other cases, CCD photometric data obtained with the Johnson V and Kron–Cousins I filters were supplemented with CCD or photoelectric Washington photometric data to determine the cluster fundamental parameters and, mainly, to estimate cluster metal content (see e.g. Piatti, Clariá & Ahumada 2003a, 2004b). We have favoured the observation of clusters which are interesting not only because of the derivation of their basic parameters, but also because of the possibility of studying the morphology of their red giant evolutionary phases in relation to previous results (see e.g. Clariá, Mermilliod & Piatti 1999; Mermilliod et al. 2001). Like in the present paper, CORAVEL radial velocity observations have been sometimes used to evaluate cluster membership as well as to detect spectroscopic binaries among the red giants in the cluster field (e.g. Clariá et al. 2003).

NGC 2489 (IAU designation CO754−299), also known as Cr 169 (Collinder 1931) or BH 15 (van den Bergh & Hagen 1975), is located in a moderately rich star field in Puppis at $\alpha_{2000} = 7^{\rm h}56^{\rm m}16^{\rm s}$,$\delta_{2000} = -30^\circ04'$ and Galactic coordinates $l = 246\overset{\circ}{.}7$ and $b = -0\overset{\circ}{.}8$. Ruprecht (1966) refers to this cluster as belonging to Trumpler class II-2m (Trumpler 1930). However, Archinal & Hybes (2003) recently classified it as I-2m, that is, a detached cluster with a strong central concentration and a medium range in the brightness of the stars. Old distance determinations range from 0.6 to 10 kpc (Alter, Ruprecht & Vanisek 1970), although more recent evidence places NGC 2489 between 1.2 and 4.0 kpc from the Sun.

It is somewhat surprising that such a comparatively bright open cluster has been the subject of relatively few previous studies. Lindoff & Johansson (1968, hereafter LJ68) performed *UBV* photographic photometry of stars brighter than $V = 15$ in the cluster field

⋆E-mail: andres@iafe.uba.ar (AEP); claria@mail.oac.uncor.edu (JJC); Jean-Claude.Mermilliod@obs.unige.ch (J-CM); celeste@mail.oac.uncor.edu (MCP); andrea@mail.oac.uncor.edu (AVA)

and derived the following parameters: $E(B-V)=0.40$, $d=1.2$ kpc and $t=250$ Myr. Although these authors do not specify the size of the errors associated with these parameters, the systematic trends in their data (see Fig. 2) and the large scatter in their (V, $B-V$) CMD produce great uncertainties and make the derived parameters unreliable. Nevertheless, LJ68's estimate of the cluster parameters is not very different from the results obtained by other authors later on.

NGC 2489 has a comparatively small angular diameter of about 5 arcmin (Lyngå 1987) quite appropriate for CCD camera analysis. However, the only *UBV* CCD photometric study up to this date was performed by Ramsay & Pollaco (1992, hereafter RP92). They obtained *UBVIc* data only in the innermost cluster area (2.2×3.3 arcmin^2) and found $E(B-V)=0.45\pm0.03$, $d=1.45\pm0.10$ kpc and $t=300$ Myr. In order to determine reddening and hence distance, RP92 applied mainly the Q method, using for such purpose the relation $E(U-B)/E(B-V)=0.72+0.05E(B-V)$. Note that RP92 obtained $(U-B)$ colours for only 37 stars situated in the innermost region of the cluster. Out of them, about 30 per cent are not cluster members according to the membership criteria defined by RP92. What is more, the cluster age reported by them should be taken only as an estimate since it was derived comparing the position of seven cluster turn-offs with only one solar isochrone computed by Vandenberg (1985) for 300 Myr. We believe that the small number of stars used to determine reddening, the fact that they belong to the innermost cluster area and the method used by RP92 to determine the cluster parameters, justify their redetermination.

Loktin et al. (2001, hereafter LGM01) published a second version of their Open Cluster Catalogue (Loktin & Matkin 1994) in which they reviewed the fundamental parameters of 423 clusters. Their updated distances are now based on a Hyades distance modulus of 3.27, being this value 0.06 mag smaller than that found from *Hipparcos* parallaxes, namely $(m-M)_V=3.33$ (Perryman et al. 1998). LGM01 determined the following parameters for NGC 2489: $E(B-V)=0.374$, $d=3957$ pc and $t=18$ Myr, which are certainly very different from those previously obtained by LJ68 and RP92. More recently, Kharchenko et al. (2005) reported practically the same cluster parameters as LGM01. A simple inspection of the (V, $B-V$) CMD of RP92 shows, however, that at least the age derived by LGM01 and Kharchenko et al. (2005) is not reliable.

NGC 2489 is also particularly interesting for the number of red giant candidates it contains as well as for the possibilities they provide in terms of cluster metal content derivation. Clariá, Piatti & Osborn (1996, hereafter CPO96) obtained photoelectric *UBV* and *DDO* photometry for six red giant candidates in the cluster area. By applying two photometric criteria described by Clariá & Lapasset (1983), they confirmed that five from the six red stars they observed are very likely cluster members and they derived $E(B-V)=0.40$ from two of them. Unfortunately, however, only one of them (no. 14 of LJ68) falls within the range of the *DDO* metallicity calibration given by Piatti, Clariá & Minniti (1993). The derived *DDO* ΔCN index for this star implies [Fe/H] = 0.0, if equation (8) of Piatti et al. (1993) is used. On the other hand, using the CPO96 data and a revised *DDO* calibration on two giants, not on one as in CPO96, Twarog, Ashman & Anthony-Twarog (1997) got [Fe/H] $=0.08\pm0.01$. Moreover, these authors did a main-sequence fit to the RP92 data to obtain a cluster distance of 1.7 kpc. Paunzen & Maitzen (2001) observed 59 stars in the Δa CCD system (V, a, g_1-y) and found four peculiar objects in the cluster field. More recently, McSwain & Gies (2005) observed 487 stars with the Strömgren band y filter as well as with a narrow-band H_α filter, looking for Be stars. None was found. With the filters observed and colours used, the authors of these two studies were certainly unable to derive an independent value for $E(b-y)$ or $E(g1-y)$ and computed the colour excesses from the value of $E(B-V)$ of LJ68.

Section 2 describes the observational material and the data reduction. The data quality as well as some structural cluster features such as the extension of the core radius and the cluster corona are discussed in Section 3. In Section 4 we describe the main features of the two CMDs, while in Section 5 through the fitting of theoretical isochrones, we determine the cluster parameters reddening, distance and age. In Section 6, the present CORAVEL radial-velocity data of red giant candidates are used to discuss cluster membership and to detect spectroscopic binaries among the red giants. In Section 7 we briefly examine the properties of a sample of known open clusters located towards the direction of NGC 2489, using the WEBDA Open Cluster Database (Mermilliod & Paunzen 2003). A summary of our main conclusions is given in Section 8.

2 THE OBSERVATIONAL MATERIAL

2.1 CCD *BVI* photometric data

CCD images of the cluster field were obtained with the Johnson B and V and Kron–Cousins I filters using the 0.9-m telescope at Cerro Tololo Inter-American Observatory (CTIO, Chile) on 2000 December 23–24. The telescope was equipped with the 2048×2048 pixel Tektronix 2K no. 3 CCD, and the seeing was typically 1.0 arcsec during the observing night. The detector used has a pixel size of 24 μm, producing a scale on the chip of 0.4 arcsec pixel^{-1} (focal ratio f/13.5) and a 13.6×13.6 arcmin^2 field of view. The CCD was controlled by the CTIO ARCON 3.3 data acquisition system in the standard quad amplifier mode, operating at a mean measured gain (four chips) of (2.00 ± 0.04) e$^-$ ADU^{-1}, with a mean readout noise of (3.60 ± 0.15) e$^-$. We obtained one 200-s, two 60-s and two 20-s V-band exposures, two 360-s, two 60-s and two 20-s B-band exposures and one 90-s and three 10-s I-band exposures for NGC 2489. The observations were supplemented with a series of 10 bias and five dome and sky flat-field exposures per filter during the observing night to calibrate the CCD instrumental signature. Standard stars of selected areas 98 and 101 of Landolt (1992), covering a wide colour range, were also observed during the night to standardize our photometry. In particular, stars in selected area 98 were observed at low and high airmasses in order to properly adjust the extinction coefficients. In total, we obtained 18 different measures of magnitude per filter for the selected standard star sample.

The *BVI* images were reduced at the Observatorio Astronómico de la Universidad Nacional de Córdoba (Argentina) with IRAF[1] using the QUADPROC package. The images were bias-subtracted and flat-fielded by employing weighted combined signal-calibrator frames. In addition, we checked the chip for the existence of any illumination pattern: no correction was necessary. Then the instrumental magnitudes for the standard fields were derived from aperture photometry using DAOPHOT/IRAF routines (Stetson, Davis & Crabtree 1990). Since there are as many instrumental magnitudes per filter as observations of standard stars, we used least squares to fit the relationships between instrumental and standard magnitudes

[1] IRAF is distributed by the National Optical Astronomy Observatories, which is operated by the Association of Universities for Research in Astronomy, Inc., under contract with the National Science Foundation.

Table 1. CCD *BVI* data of stars in the field of NGC 2489. The full version of this table is available in the online version of this article.

Star	x (pixel)	y (pixel)	V (mag)	$\sigma(V)$ (mag)	$B-V$ (mag)	$\sigma(B-V)$ (mag)	$V-I$ (mag)	$\sigma(V-I)$ (mag)	n
1609	1273.297	376.256	14.569	0.013	0.508	0.015	0.649	0.020	1
1610	754.474	377.191	16.158	0.012	0.976	0.009	1.349	0.018	3
1611	690.234	386.242	18.319	0.005	1.359	0.055	1.921	0.006	2
...	...	...	...	...	...	...	...	...	...
...	...	...	...	...	...	...	...	...	...

Note: (x, y) coordinates correspond to the reference system of Fig. 1. Magnitude and colour errors are the s.d. values of the mean, or the observed photometric errors for stars with only one measurement. Only for those stars with CORAVEL radial-velocity data, numbers in the LJ68's numbering system are given in parenthesis in the first column.

simultaneously and we obtained the following results:

$$v = (2.003 \pm 0.008) + V + (0.123 \pm 0.004) \times X_V - (0.030 \pm 0.007) \times (B - V), \quad (1)$$

$$b = (2.176 \pm 0.026) + V + (B - V) + (0.237 \pm 0.121) \times X_B + (0.066 \pm 0.021) \times (B - V), \quad (2)$$

$$i = (2.899 \pm 0.008) + V - (V - I) + (0.058 \pm 0.005) \times X_I - (0.017 \pm 0.005) \times (V - I), \quad (3)$$

where X represents the effective airmass. The coefficients were derived through the IRAF routine FITPARAM. Capital and lowercase letters represent standard and instrumental magnitudes, respectively. We then derived the instrumental magnitudes for stars in the NGC 2489 field from point spread function fits using stand-alone versions of the DAOPHOT[2] and ALLSTAR[2] programs. Before transforming the magnitudes into the standard system, we combined all the independent measurements in three different tables using the stand-alone DAOMATCH[2] and DAOMASTER[2] programs. The columns in these tables list a running number, the x and y coordinates, the v, b and i magnitudes, and the respective observational error for each measured star. Once we obtained the standard magnitudes and colours, we built a master table containing the average of $V, B-V$ and $V-I$, their errors $\sigma(V)$, $\sigma(B-V)$ and $\sigma(V-I)$, and the number of observations for each star, respectively. Whenever there exists only one measure of $V, B-V$ and/or $V-I$, we adopted the corresponding observational error. We derived magnitudes and colours for 2182 stars in the field of NGC 2489, which are provided in Table 1. A fragment of this table is shown here for guidance regarding its form and content, its entirety being available in the online version of the journal on *Synergy*. Only for those stars with CORAVEL radial-velocity data (see Section 2.2), numbers in the LJ68's numbering system are given in parenthesis in the first column of Table 1. Fig. 1 shows a schematic finding chart of the stars observed in the field of NGC 2489. The sizes of the plotting symbols are proportional to the V brightness of the stars.

A total of 111 stars observed at CTIO in the *BV* system were also measured photographically by LJ68 but they do not show good agreement in general terms. In fact, Fig. 2 (left-hand panels) shows that not only an important zero-point difference exists between both magnitude scales, but there is also a trend of increasing their difference towards fainter magnitudes. On the other hand, the mean differences and s.d. values for five cluster giants observed photoelectrically by CPO96 – we adopted these measurements for these stars instead of the CCD ones – are $\Delta V(\mathrm{CPO96}-\mathrm{LJ68}) = -0.05 \pm 0.04$, $\Delta(B-V)(\mathrm{CPO96}-\mathrm{LJ68}) = 0.07 \pm 0.03$, which means that even at that bright magnitude level, there exist distinguishable differences. A better agreement results when comparing our V data with the CCD ones of RP92 for 60 stars measured in common, being now the mean difference ΔV (ours − RP92) $= -0.01 \pm 0.06$. However, the difference $\Delta(B-V)$ (ours − RP92) is clearly not a linear function of V (see Fig. 2, right-hand panels). This difference reaches nearly −0.10 for stars in range $14 < V < 18$, the region where the RP92's fit is done. This fact explains the difference between the $E(B-V)$ values derived here and that derived by RP92 (see Section 5). The $(V-I)$ colour indices of RP92 are also clearly redder than ours.

The mean difference is $\Delta(V-I)$(ours − RP92) $= -0.14 \pm 0.06$. These differences are significant and will largely explain the differences between the cluster parameters published by RP92 and those derived in the present study.

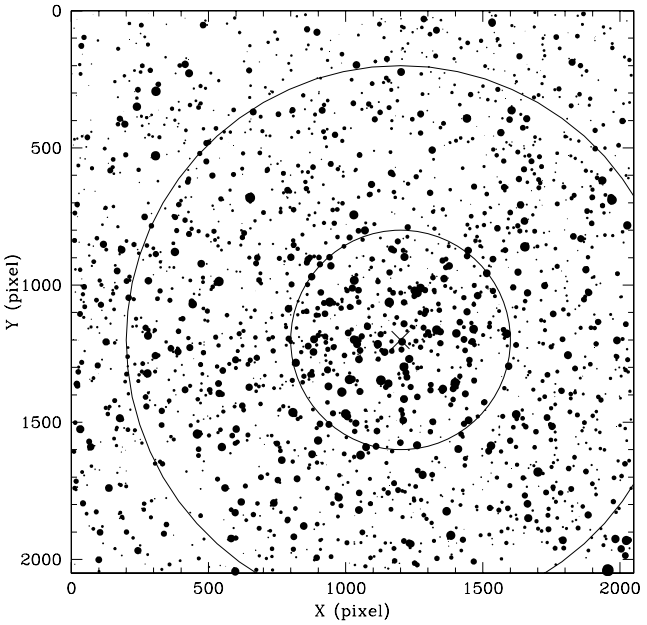

Figure 1. Schematic finding chart of the stars observed in the field of NGC 2489. North is up and east is to the left-hand side. The sizes of the plotting symbols are proportional to the V brightness of the stars. Two concentric circles 400 and 1000 pixels wide around the cluster centre (cross) are shown.

[2] Program kindly provided by P. B. Stetson.

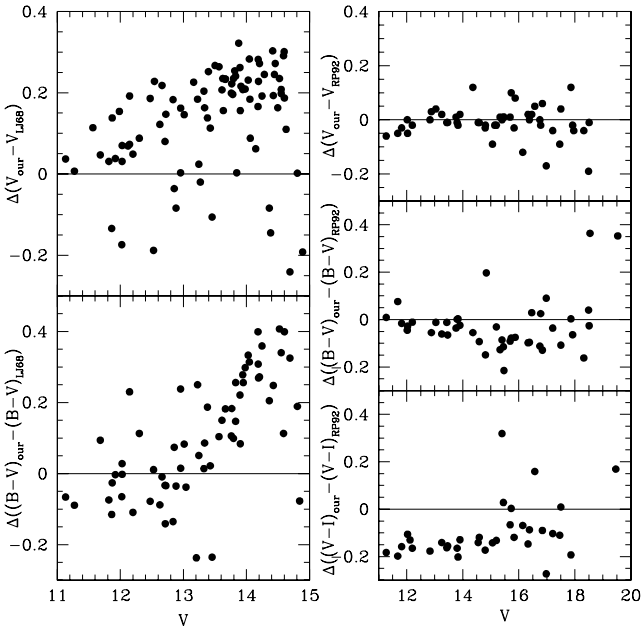

Figure 2. Magnitude and colour differences between our values and those by LJ68 for 111 stars in common (left-hand panels) and our values and those by RP92 for 60 stars in common (right-hand panels) as a function of *V*.

2.2 Radial velocity observations

Seven stars in the cluster field brighter than $V = 12.20$ and redder than $B - V = 1.20$ were originally selected as red giant candidates of NGC 2489 from the CMD published by LJ68. Radial-velocity observations were obtained for these seven red giant candidates with the CORAVEL instrument (Baranne, Mayor & Poncet 1979) at the 1.54-m Danish telescope at European Southern Observatory (ESO), La Silla, Chile. A total of four observations per star were obtained successively in 1984, 1986, 1989 and 1994 for the single stars during the course of a long-term systematic programme. The radial velocities are on the system defined by Udry, Mayor & Queloz (1999) from high-precision radial-velocities obtained with the ELODIE spectrograph (Baranne et al. 1996). This calibration corrects all systematic errors of the CORAVEL system.

Our mean results for individual stars in NGC 2489 are summarized in Table 2, which gives the star number from LJ68, the mean radial velocity and its uncertainty, the dispersion in the mean radial velocities – both in (km s^{-1}) – the ratio of the external to internal errors (E/I), the number of radial-velocity observations, the probability P(χ^2) that the scatter is due to random noise, the time interval in days covered by the observations of each star, and some remarks about membership and duplicity (SB = spectroscopic binary). The individual radial-velocity observations will be published in a comprehensive catalogue of all CORAVEL cluster red giant radial velocities (Mermilliod & Mayor, in preparation). They may also be requested directly from JCM.

Table 2. CORAVEL radial-velocity data.

Star	V_r	ϵ	σ	*E/I*	*N*	$P(\chi^2)$	ΔT	Notes
3	+46.32	0.20	0.20	0.45	5	0.936	3973	NM
14	+38.27	0.27	0.28	0.51	4	0.859	3608	M
25	+38.35	0.16	8.15	14.91	24	0.000	4330	M, SB
36	+37.90	0.48	0.96	1.36	4	0.140	3608	M
37	+38.01	0.22	0.25	0.55	4	0.821	3608	M
50	+38.63	0.28	0.04	0.07	4	0.999	3610	M
103	+37.61	0.29	0.46	0.79	4	0.605	3610	M

3 DATA HANDLING

3.1 Data quality and scopes

On examining Table 1, it is found that more than 50 per cent of the total measured stars have $V - I$ colours and *V* magnitudes ranging from ∼19 down to 22 mag. The remaining measured stars satisfy that 9 per cent of them with $B - V$ and $V - I$ colours have, respectively, three measures, and expand from the brightest down to the faintest limits in the (V, $B - V$) CMD (see Fig. 5). Two measures of $B - V$ and $V - I$ colours occur for the 19 per cent of the stars and cover *V* ranges similar to those stars with three measures in both colours. One measure in $B - V$ and $V - I$ applies to 16 per cent of the stars, all of them being fainter than ∼14 mag down to the photometric magnitude limit. According to this crude statistics, most of the ∼8 mag along which our photometry extends in the (V, $B - V$) CMD, is covered by stars measured once and twice. At the same time, we have approximately 56 per cent of the measured stars distributed within the two faintest magnitudes reached (see Fig. 6). Such a result reveals that the field of NGC 2489 has plenty of relatively faint stars, which probably constitute the cluster background.

In Fig. 3 we plotted the photometric errors provided by the s.d. of the mean for the *V* magnitude and $B - V$ and $V - I$ colours against their corresponding *V* magnitudes. We used all the measured stars, without distinguishing between stars measured once, twice or three times. By using photometric errors provided by DAOPHOT (only one measure per star), we obtained similar diagrams with a reasonably smaller intrinsic scatter. With the knowledge of the behaviour of the photometric errors with the magnitude for these stars provided in Fig. 3, we rely on the accuracy of the morphology and position of the main cluster features in the CMDs.

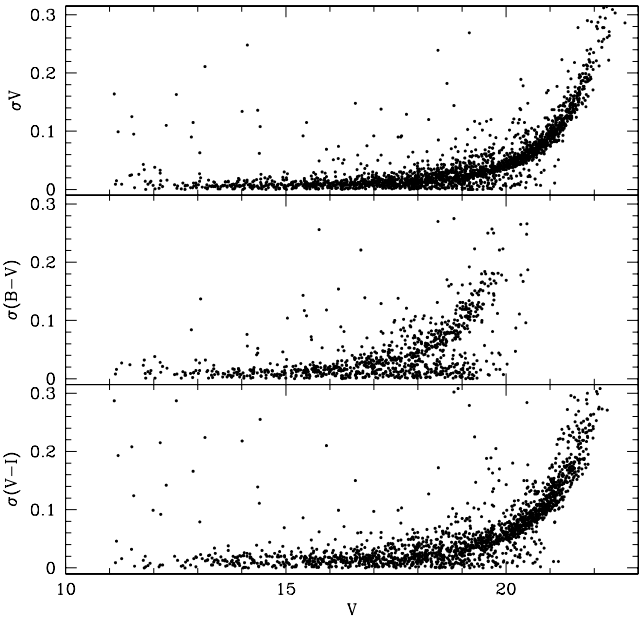

Figure 3. Magnitude and colour photometric errors as a function of *V*.

3.2 Structural cluster features

Because the exact position on the cluster centre cannot be easily determined by eye examination, we defined a strategy to determine it statistically. We traced the stellar density profiles projected on to the direction of the *x*- and *y*-axes to obtain the coordinates associated to the peak of the stellar density distribution by fitting those profiles. We counted the number of stars distributed along bands of a fixed width and oriented along the *y*-axis in order to build the *x* projected density profile, and we used bands placed along the *x*-axis to construct the *y*-projected density profile. The width of the bands was fixed in 50, 100 and 150 pixels for both axes. These values were chosen to check the behaviour of spurious effects, mainly caused by the presence of localized groups, rows or columns of stars, and thus to select the one which most appropriately fits the spatial resolution. Note that the range of useful bin sizes is also constrained by the mean field stellar density, which results in a lower limit for the mean free path between two stars. We chose relatively large intervals because the field is not too crowded. We found that with the 50 pixel bins, the profiles resulted noisy, whereas with the 150 pixel bins they were smooth. Thus, we finally adopted a bin size of 100 pixels in the subsequent analysis.

We fitted the projected stellar density profiles using the NGAUSSFIT routine of the STSDAS IRAF package. The multiple Gaussian fitting option was adopted. It fixed the constant and linear terms to the corresponding background level and to zero, respectively, and set the number of matching Gaussians to one. The centre of the Gaussian, its amplitude and its full width at half-maximum acted as variables. After eliminating a couple of scattered points, the fitting procedure converged with one iteration on average. The resulting values were compared with the cluster centre which was estimated by eye while looking at the cluster finding chart. The final coordinates for the cluster centre, marked by a cross in Fig. 1, turned out to be $(x_c, y_c) = (1200 \pm 100, 1200 \pm 100)$ pixels, which were adopted for the following analysis.

We then built the cluster stellar density radial profile. The most common way of building such radial profile is to count the number of stars distributed in concentric rings around the cluster centre and to normalize the sum of stars in each ring to the unit area. Following this procedure it is easy to trace the radial profile as long as complete circles can be traced in the observed field. However, one can move even further away from the cluster centre on the basis of counts of stars located in boxes of 100 pixels a side, which are spread throughout the whole field. Thus, the number of stars per unit area at a given radius *r* can be directly calculated through the expression

$$\frac{n_{r+50} - n_{r-50}}{(m_{r+50} - m_{r-50}) \times 100^2},$$

where n_j and m_j, respectively, represent the number of counted stars and centres of boxes of 100 pixels a side included in a circle of radius *j*. Fig. 4 depicts the resulting stellar density profile. Note that in order to estimate the mean stellar density at that distance, this method does not necessarily require a complete circle of radius *r* within the observed field. Moreover, with this method we reached up to 1700 pixels from its centre, instead of tracing the radial profile of NGC 2489 out of ∼800 pixels (the radius of the largest complete circle that can be traced in the observed field).

The resulting cluster radial profile allows us to reach multiple aims. First, to estimate the cluster radius, generally used as indicator of the cluster dimension; secondly, to examine the extension of the cluster core and corona; and finally, to establish the area out of which field stars prevail. The availability of a field area is highly valued, mainly because it helps to disentangle fiducial cluster and field features in the observed CMDs.

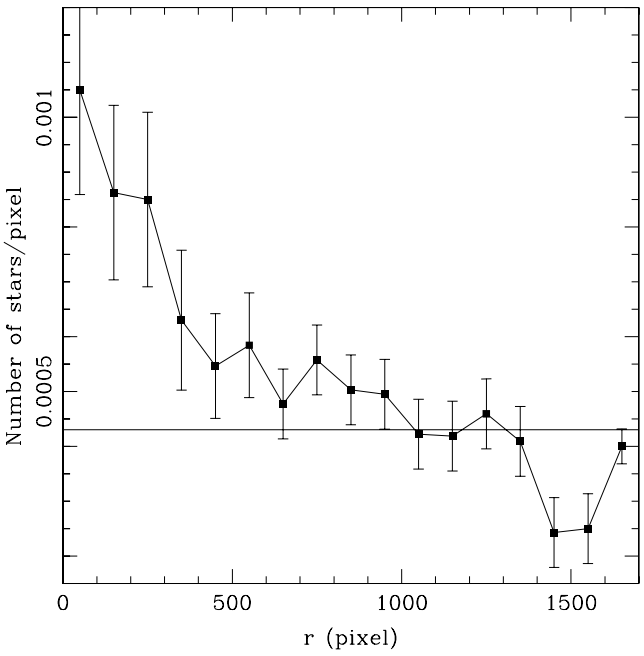

Figure 4. Stellar density profile centred at $(x_c, y_c) = (1200, 1200)$ pixels for stars observed in the field of NGC 2489. The horizontal line represents the background level measured for $r > 1000$ pixels.

With the purpose of estimating the uncertainties in the derived stellar density profile, we proceeded to build two additional radial profiles so as to count the number of the stars distributed within them using boxes of 50 and 150 pixels a side, respectively. We followed the steps described above, and the resulting s.e. values were used to draw the error bars in Fig. 4. As can be seen, the more inwards a radius, the longer the error bars. This is due to the non-uniform distribution of cluster stars.

The mean stellar density in the outermost observed regions proves to be slightly lower than half of the central cluster density. The horizontal line at 0.000 43 pixels^{-1} in Fig. 4 represents the derived background level, which was fixed using the error bars as a secondary reference. From this figure, we also estimated a cluster radius of 1000 ± 100 pixels, equivalent to 6.7 ± 0.6 arcmin, and adopted the region for $r > 1000$ pixels as the 'star field area'.

Note that the main body of NGC 2489 is confined to a radius of ∼400 pixels (∼2.7 arcmin) and that a faint corona extends up to the cluster boundary (see also Fig. 1). We compared the cluster density profile with those of other clusters observed using both the same CCD and the same telescope, having previously normalized the respective field star densities. We found that NGC 2489 has an intermediate star density, like NGC 2194 (Piatti et al. 2003a), NGC 2324 (Piatti et al. 2004b), Tombaugh 1 (Piatti, Clariá & Ahumada 2004c) and Lyngå 11 (Piatti et al. 2006a), which are between the highest density clusters NGC 6318 (Piatti, Clariá & Ahumada 2005) and Tr 5 (Piatti, Clariá & Ahumada 2004a) and the lowest density cluster NGC 5288 (Piatti et al. 2006b). Regarding the shape of the NGC 2489 density profile, it compares well at the core with those of clusters of intermediate star densities, but shows additionally a corona not so extended as that of NGC 5288. In fact, the ratio between the annular width of the corona and the core radius in NGC 2489 is 1.5, while the average value found by Nilakshi,

Pandey & Mohan (2002) for 38 open clusters is 4.3 ± 1.9. However, a large sample of star clusters is required to understand the cause of the variations in the profile.

4 COLOUR–MAGNITUDE DIAGRAM FEATURES

The resulting $(V, B-V)$ and $(V, V-I)$ CMDs obtained using all the measured stars are depicted in Figs 5 and 6, respectively. On looking simultaneously at both figures, one first captures the difference in the magnitude dynamical ranges; the $(V, V-I)$ CMD containing many more stars fainter than $V \approx 19$ and down to 3 mag below. This amount of stars represents more than 50 per cent of the total number of measured stars, far from the expected relative number of stars of the cluster star luminosity function in that magnitude interval. They could probably be field stars. The figures reveal well populated and relatively narrow sequences of stars that trace the cluster main sequence (MS) along ∼7 mag with clear evidence of some evolution. This fact suggests that the age of the cluster should be some hundred million years old. A clump of red stars is also clearly visible.

The width of the cluster MS seems to be mainly intrinsic, since the scatter produced by photometric errors does not reach a tenth of magnitude at $V = 20$. Furthermore, according to Fig. 3, $\sigma_V \leqslant 0.05$ mag for $V = 19$ and ≈0.01 mag for $V < 17$; $\sigma_{B-V} \leqslant 0.05$ mag for $V = 18$ and 0.01 mag for $V < 16$ and $\sigma_{V-I} \leqslant 0.05$ mag for $V = 18.5$ and 0.01 mag for $V < 16.5$.

Field star contamination in the core ($r < 400$ pixels) and in the corona ($400 < r < 1000$ pixels) results on average ∼50 and 90 per cent, respectively. Although the corona has an annular radius 1.5 times larger than the radius of the central cluster region (see Fig. 4), it contains no more than ∼35 per cent of the cluster stars because of its relatively low star density. Taking into account both reasons, we used the $r < 400$ pixels CMDs in the estimation of the cluster fundamental parameters to guarantee the presence of a predominant number of cluster stars over field stars.

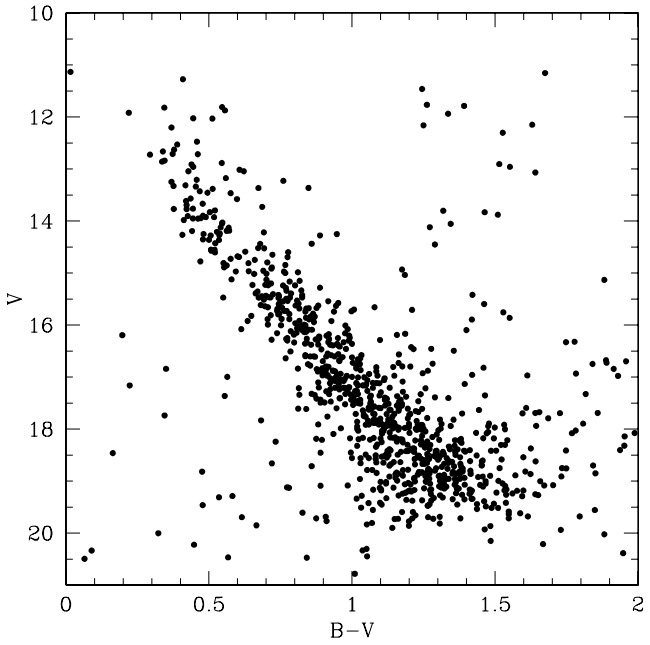

Figure 5. $(V, B-V)$ CMD for stars observed in the field of NGC 2489.

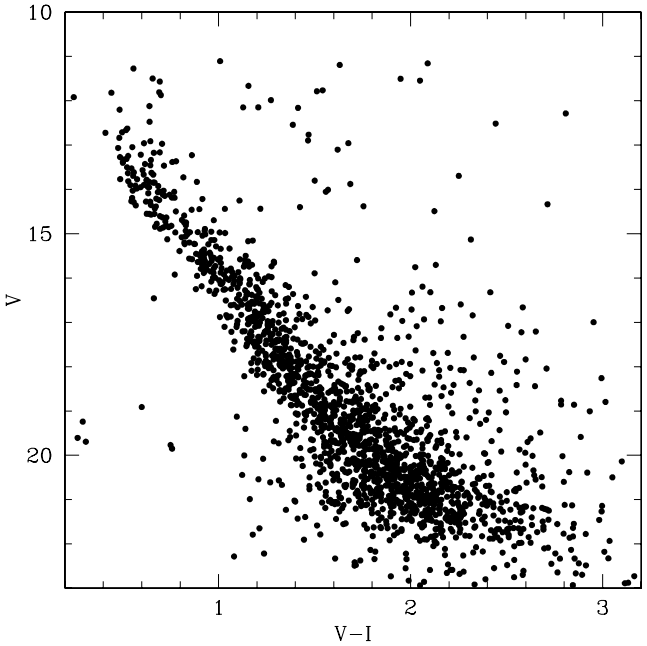

Figure 6. $(V, V-I)$ CMD diagram for stars observed in the field of NGC 2489.

5 CLUSTER FUNDAMENTAL PARAMETER ESTIMATES

We fitted theoretical isochrones to the observed CMDs to estimate the $E(B-V)$ and $E(V-I)$ colour excesses, the $V - M_V$ apparent distance modulus and the age of NGC 2489. The theoretical isochrones computed by Girardi et al. (2002) were used instead of those of Lejeune & Schaerer (2001) – generally used in previous papers of ours (see Section 1) – since the former were calculated for fainter magnitudes. When selecting subsets of isochrones, we preferred those including overshooting effect. Since the only previous available estimates of the cluster metal content are those of Twarog et al. (1997) and CPO96, we adopted a chemical composition of $Z = 0.019$ ([Fe/H] = 0.0) for the isochrone sets.

We first looked for clusters with similar CMDs. The morphology of the $(V, B-V)$ sequence and the width of the Hertzsprung gap closely resemble the characteristics of Praesepe (NGC 2632) sequence. Matching the sequences of both clusters yielded first estimates of reddening, distance modulus and age, which were close to the values finally adopted. Because the sequence in the $(V, V-I)$ CMD reaches fainter magnitudes and is better delineated, we first estimated the cluster parameters by fitting the isochrone on this CMD to derive both the cluster colour excess $E(V-I)$ and the apparent distance modulus $V - M_V$. Note that the typical curvatures of the lower portions of the unevolved MS are clearly seen in the $(V, V-I)$ CMD. This is not the case in the $(V, B-V)$ CMD, in which the above curvatures do not appear as clearly defined as in the $(V, V-I)$ CMD, probably due to photometric errors, among other causes. Fig. 3 shows that $\sigma_{(B-V)}$ is almost twice $\sigma_{(V-I)}$ for $17 < V < 19$. In the case of the observed unevolved MS in the $(V, V-I)$ CMD of NGC 2489, its extension and shape allowed us to obtain a couple of $E(V-I)$ and $V - M_V$ values, with their respective errors. These errors arise from the width of the MS, which is mainly caused by photometric errors and/or intrinsic scatter. We thus derived $E(V-I) = 0.40 \pm 0.05$ and $V - M_V = 12.20 \pm 0.25$. Then, we adopted the estimated apparent distance modulus and looked for the

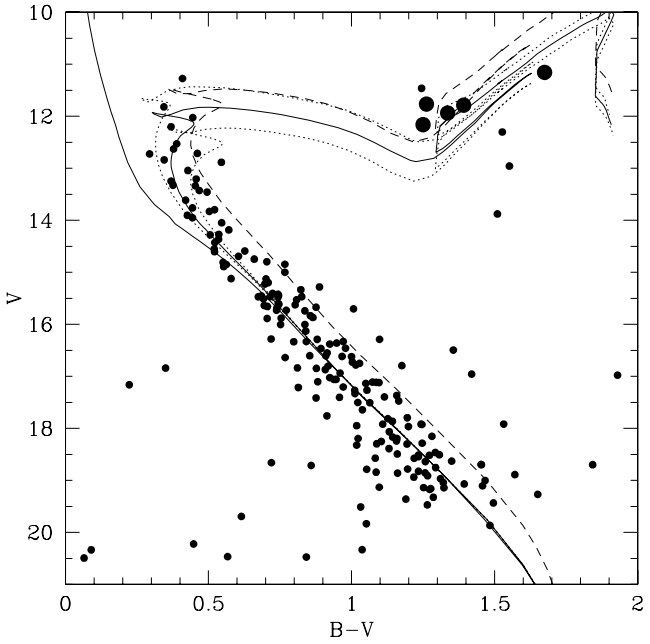

Figure 7. $r < 400$ pixels ($V, B-V$) CMD for stars in NGC 2489. The ZAMS and the isochrone of $\log t = 8.70$ from Girardi et al. (2002), computed taking into account overshooting and $Z = 0.019$, are overplotted (solid lines). Two additional isochrones for $\log t = 8.6$ and 8.8 are also drawn for comparison purposes (dotted lines). The dashed curve is the isochrone of $\log t = 8.70$ shifted by 0.75 mag to reproduce the upper binary ridge. The large filled circles correspond to cluster giant members 14, 25, 36, 37 and 50 in the LJ68's numbering system.

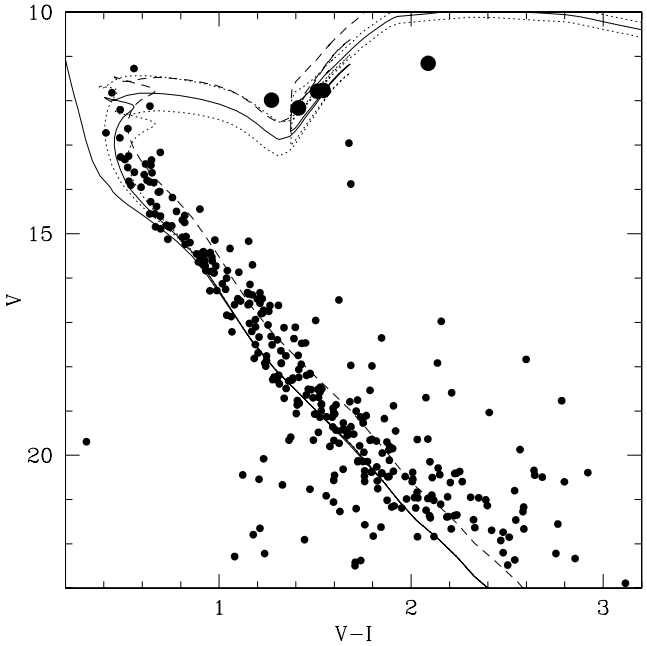

Figure 8. $r < 400$ pixels ($V, V-I$) CMD for stars in NGC 2489. The ZAMS and the isochrone of $\log t = 8.70$ from Girardi et al. (2002), computed taking into account overshooting and $Z = 0.019$, are overplotted (solid lines). Two additional isochrones for $\log t = 8.6$ and 8.8 are also drawn for comparison purposes (dotted lines). The dashed curve is the isochrone of $\log t = 8.70$ shifted by 0.75 mag to reproduce the upper binary ridge. The large filled circles correspond to cluster giant members 14, 36, 37, 50 and 103 in the LJ68's numbering system.

corresponding $E(B-V)$ colour excess by shifting in colour the theoretical zero-age main-sequence (ZAMS) on to the observed cluster ($V, B-V$) CMD until we obtained a satisfactory fit of the unevolved cluster MS. We estimated $E(B-V) = 0.30 \pm 0.05$, which in turn leads to a $E(V-I)/E(B-V)$ ratio in excellent agreement with that coming from the normal interstellar extinction law (=1.25; Dean, Warren & Cousins 1978). Note that we could have adopted a value for the $E(V-I)/E(B-V)$ ratio first and then checked that the fit of the ZAMS in the (V, $B-V$) CMD was consistent with the other one.

Next, we selected isochrones of $\log t$ larger than 8.0 and used the derived $V - M_V$ and $E(V-I)$ values to estimate the cluster age. The isochrone of $\log t = 8.70$ ($t = 500$ Myr) turned out to be the one which most accurately reproduces the cluster features in the (V, $V-I$) CMD. The presence of a red giant clump in the cluster CMD made the fitting procedure easier. As an additional constraint to adopt a cluster age, we made sure there was coherence with the isochrone fit in the (V, $B-V$) CMD. Finally, we estimated the uncertainty of the derived age as $\sigma_{\log t} \pm 0.1$ ($\sigma_t = {}^{+130}_{-100}$). In Figs 7 and 8 we overlapped the ZAMS and the isochrone of $\log t = 8.70$ (solid lines) for $Z = 0.019$ to the cluster CMDs. Two additional isochrones for $\log t = 8.6$ and 8.8 were also drawn for comparison purposes (dotted lines) in both figures. The dashed line in each of them represents the same isochrone of $\log t = 8.7$, shifted by 0.75 mag to reproduce the upper binary ridge. As shown in these figures, the morphology of the turn-off point (ZAMS and binary ridge) is well reproduced.

We also checked that the fundamental parameters derived for the cluster do not depend on the adopted theoretical isochrone. In previous papers, we used the isochrones of Lejeune & Schaerer (2001),

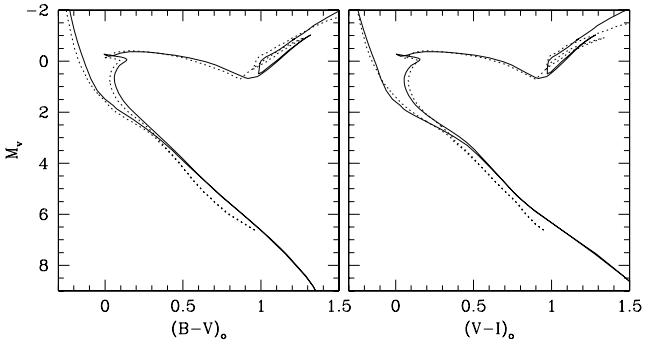

Figure 9. Comparison between the isochrones computed by Girardi et al. (2002, solid lines) and by Lejeune & Schaerer (2001, dotted lines) for $Z = 0.019$ and $\log t = 8.7$.

which provided ages on a uniform scale. Fig. 9 shows the isochrones of Girardi et al. (solid lines) and Lejeune & Schaerer (dotted lines), computed for $Z = 0.019$ and $\log t = 8.7$, superimposed. We decided to use Girardi et al. isochrones because they were calculated for fainter magnitudes and, therefore, allowed us to fit the lower end of the cluster MS better. A very good agreement is clearly seen between both isochrones, which means that the age of NGC 2489 is in the same age scale as the one of the previously studied clusters.

We used the derived reddenings and apparent distance modulus and the most frequently used value for the $A_V/E(B-V)$ ratio (Straizys 1992) to obtain a true distance modulus $V_o - M_V = 11.24 \pm 0.40$, which implies a distance from the Sun of (1.8 ± 0.3) kpc and 25 pc below the Galactic plane. The distance error was

computed with the expression: $\sigma(d) = 0.46 \times [\sigma(V - M_V) + 3.2 \times \sigma(E(B-V))] \times d$, where $\sigma(V - M_V)$ and $\sigma(E(B-V))$ represent the estimated errors in $V - M_V$ and $E(B - V)$, respectively. By using the Galactic coordinates (l, b) and distance of the cluster, we derived (9.21, −1.65, −0.03) kpc and ∼9.4 kpc for the Galactic (X, Y, Z) coordinates and Galactocentric distance, respectively, assuming the Sun's distance from the centre of the Galaxy to be 8.5 kpc.

The cluster fundamental parameters here derived show differences from those derived in previous papers (see Section 1), even if we compare our results with the ones obtained by RP92. Although the distances inferred both by RP92 and by us show a reasonable agreement within the error bars, our $E(B - V)$ colour excess turns out to be 0.15 mag smaller, while the cluster age here estimated is about a factor of 2 larger than that of RP92. The significant difference in $E(B - V)$ arises mainly from the difference in the $B - V$ colour scale for stars in range $14 < V < 18$ (see Fig. 2, right-hand panels), precisely the region where the fits are done. The discrepancy between the $E(B - V)$ values could also be partly explained considering that RP92 obtained CCD data only for 120 stars located within an area of 2.2×3.3 arcmin^2 in the sky, whereas we measure a total of 2182 stars within an area twenty five times larger. Finally, it should be remarked that the inferred distance in this work (1.8 kpc) is very similar to the one 1.7 kpc value obtained by Twarog et al. (1997) from the fit to the RP92 data.

6 RED STARS IN THE CLUSTER FIELD

Based on the CORAVEL data (Table 2), six out the seven red stars observed can be treated as unarguable members of NGC 2489, since their radial velocities exhibit very close agreement. The mean radial velocity from these stars is 38.13 ± 0.33 km s^{-1} and has been adopted for the cluster. Star 25 is a single-lined SB whose orbit has been determined by Mermilliod, Andersen & Mayor (1997). Its systemic velocity differs by only 0.16 km s^{-1} from the cluster mean velocity. This star is then undoubtedly a member of NGC 2489.

Cluster membership among the possible red giants was also examined by CPO96, who obtained high-precision *UBV* and *DDO* data for six of the seven stars here observed with the CORAVEL. Their results are based on two photometric criteria defined by Clariá & Lapasset (1983) and show very good agreement with those coming from the present CORAVEL radial-velocity data.

7 NGC 2489: A FINAL ASSESSMENT

Our resulting age confirms that NGC 2489 is a Hyades-like open cluster of ∼500 Myr and not a very young object as LGM01 and Kharchenko et al. (2005) claim. According to the metallicity estimated by Twarog et al. (1997) and CPO96, the cluster fits well in the expected locus in the position–metallicity relationship (see e.g. Chen, Hou & Wang 2003).

In the general framework of the structure and evolution of the Galactic disc, NGC 2489 does not appear to have an unexpected behaviour. To confirm such assertion, we first searched for clusters located at $(l, b)_{\rm cluster} = (l, b)_{\rm NGC\,2489} \pm 5^\circ$ in order to investigate the absorption extinction law along the line of sight to NGC 2489. As far as we know, the WEBDA Open Cluster Database (Mermilliod & Paunzen 2003) is an excellent tool to analyse cluster samples, since it is updated periodically. Therefore, we searched the WEBDA for open clusters with well-determined $E(B - V)$ colour excesses and distances from the Sun. When any of such quantities was not provided by WEBDA, we appealed to the most recent literature available. We found a sample of 18 open clusters within the desired (l, b) range, out of which only 10 have some fundamental parameters and their uncertainties determined. Table 3 displays in successive columns the name of the clusters, their Galactic coordinates l and b, their distances from the Sun and their $E(B - V)$ colour excesses, together with the references from which those values were taken. The result of the search shows that further work is required to increase the number of detailed studies on open clusters.

Fig. 10 shows the relationship between the visual interstellar absorption A_V and the distance d from the Sun for the selected clusters (filled circles) and NGC 2489 (open star). First, note that the distance between the outermost and the innermost clusters is nearly 4.5 kpc. The error bars correspond to those errors provided in Table 3 for the cluster parameters. For the sake of comparison, we also included the relation between A_V and d corresponding to the Baade's Window [$(l, b) = (1^\circ, -3.9^\circ)$] – situated not far from the direction here considered – obtained by Ng et al. (1996), which is represented by a solid line. It can be seen in the same figure that from the Sun outwards up to ∼3 kpc, the clusters approximately follow the interstellar extinction law of the Baade's Window. At that distance, however, there occurs a large dispersion in the interstellar visual absorption. According to the schematic map of the Galaxy of Drimmel & Spergel (2001), there are no spiral arms passing near to these five clusters. An explanation for this scatter might be the existence of dark clouds in front of them or simply the evidence that the dust distribution in the Galactic plane is not homogeneous.

Table 3. Fundamental parameters of clusters located towards NGC 2489.

Cluster	l (°)	b (°)	d (kpc)	Reference	$E(B - V)$ (mag)	Reference
ASCC 43	244.73	−0.39	1.00 ± 0.20	1	0.10 ± 0.05	1
Haffner 21	244.85	1.63	3.30 ± 0.40	2	0.20 ± 0.04	2
Ruprecht 44	245.75	0.48	4.80 ± 0.80	3	0.58 ± 0.05	3
Czernik 32	245.89	−1.73	4.10 ± 0.90	4	0.85 ± 0.10	4
Ruprecht 43	246.06	0.39	1.30 ± 0.20	1	0.27 ± 0.05	1
Haffner 20	246.97	−0.93	2.40 ± 0.30	2	0.55 ± 0.04	2
Haffner 17	247.71	−2.53	2.88 ± 0.50	6	1.26 ± 0.04	6
NGC 2533	247.80	1.31	1.70 ± 0.30	7	0.14 ± 0.05	7
Ruprecht 47	248.25	−0.19	3.01 ± 0.20	1	0.28 ± 0.05	1
ESO 430-SC18	248.58	0.76	0.83 ± 0.20	1	0.00 ± 0.05	1

References: (1) Kharchenko et al. (2005); (2) Fitzgerald & Moffat (1974); (3) Netopil et al. (2007); (4) Carraro et al. (2005a); (6) Pedreros (2000); (7) Carraro et al. (2005b).

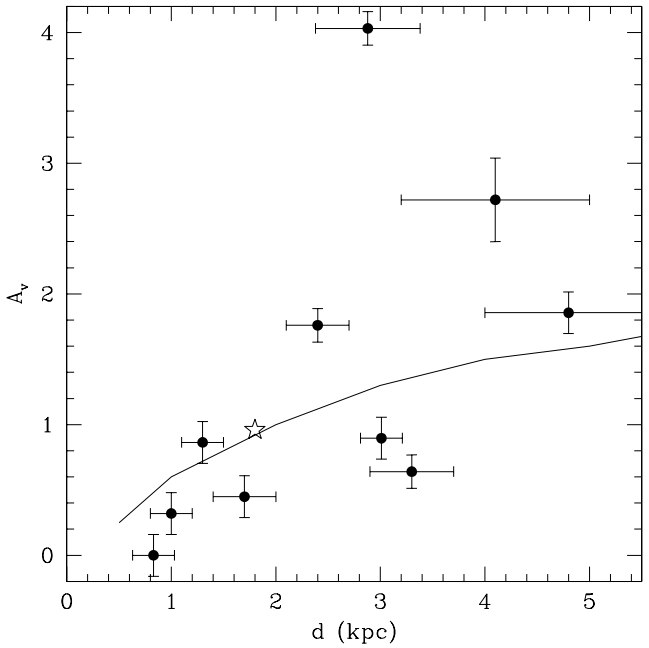

Figure 10. Relation between the distance from the Sun and the visual interstellar absorption for known open clusters located in the direction towards NGC 2489. Selected clusters and NGC 2489 are represented by filled circles and by an open star, respectively. Error bars for the cluster parameters are also drawn. The relation corresponding to the Baade's window – situated not far from the direction to NGC 2489 – is shown as a solid line.

8 SUMMARY AND CONCLUSIONS

We present CCD observations in the Johnson B and V and Kron–Cousins I passbands for 2182 stars in the region of the southern open cluster NGC 2489 and its surrounding field. These observations have been used to build CMDs reaching down to $V \sim 21.5$. We also present CORAVEL radial velocities for seven red giant candidates. The analysis of the present photometric and kinematical data leads to the following main conclusions.

(i) From the cluster star density profile, we conclude that NGC 2489 is an intermediate star density cluster. An angular radius of 1000 ± 100 pixels, equivalent to 6.7 ± 0.6 arcmin, was estimated from star counts in 100-pixel a side boxes distributed throughout the entire observed field. Therefore, the cluster linear radius turned out to be 3.5 ± 0.3 pc. NGC 2489 appears to have a relatively small but conspicuous nucleus and a low-density coronal region, being 1.5 the ratio between the annular width of the corona and the core radius.

(ii) The observed (V, $B - V$) and (V, $V - I$) CMDs, corrected by field star contamination, reveal well populated and relatively narrow MSs extending along $\sim$7 mag. Estimates of the cluster fundamental parameters arose from the theoretical isochrones of the Padova group. For $Z = 0.019$, the best-fitting isochrones yields $E(B - V) = 0.30 \pm 0.05$, $E(V - I) = 0.40 \pm 0.05$, $V - M_V = 12.20 \pm 0.25$ and an age of (500^{+130}_{-100}) Myr. The latter is almost 30 times older than the ages recently estimated by LGM01 and Kharchenko et al. (2005) and even almost a factor of 2 larger than the value reported by RP92.

(iii) NGC 2489 is located at 1.8 ± 0.3 kpc from the Sun, 25 pc below the Galactic plane and $\sim$9.4 kpc from the Galactic Centre.

(iv) Cluster membership for six red giants has been confirmed by the analysis of the CORAVEL radial-velocity data, one of them being a spectroscopic binary. A mean cluster radial velocity of 38.13 ± 0.33 km s^{-1} was derived from these stars.

(v) An inspection of the properties of 10 well-known open clusters aligned along the line of sight to NGC 2489 as seen from the Sun reveals that all those located closer than $\sim$3 kpc follow the interstellar extinction law of Baade's window. Beyond this distance, a large dispersion occurs in the visual interstellar absorption, probably caused by the presence of isolated dark clouds.

ACKNOWLEDGMENTS

This work is based on observations made at Cerro Tololo Inter-American Observatory (CTIO), which is operated by AURA, Inc., under cooperative agreement with the National Science Foundation. The present work was partially supported by the Argentinian institutions CONICET, Agencia Nacional de Promoción Científica y Tecnológica (ANPCyT) and Agencia Córdoba Ciencia. We thanks the comments made by an anonymous referee which helped us to improve the manuscript.

REFERENCES

Alter G., Ruprecht J., Vanisek J., 1970, Catalogue of Star Clusters and Associations. Akademiai Kiado, Budapest
Archinal B. A., Hynes S. J., 2003, Star Clusters. Willman-Bell, Inc., Richmond VA
Baranne A., Mayor M., Poncet J.-L., 1979, Vistas Astron., 23, 279
Baranne A. et al., 1996, A&AS, 119, 373
Carraro G., Baume G., Vázquez R. A., Moitinho A., Geisler D., 2005a, MNRAS, 362, 649
Carraro G., Vzquez R. A., Moitinho A., Baume G., 2005b, ApJ, 630, L153
Chen L., Hou J. L., Wang J. J., 2003, AJ, 125, 1397
Clariá J. J., Lapasset E., 1983, JA&A, 4, 117
Clariá J. J., Piatti A. E., Osborn W., 1996, PASP, 108, 672 (CPO96)
Clariá J. J., Mermilliod J.-C., Piatti A. E., 1999, A&AS, 134, 301
Clariá J. J., Piatti A. E., Lapasset E., Mermilliod J.-C., 2003, A&A, 399, 543
Collinder P., 1931, Medd. Lunds. Astron. Obs., 2, 1
Dean F. J., Warren P. R., Cousins A. W. J., 1978, MNRAS, 183, 569
Drimmel R., Spergel D. N., 2001, ApJ, 556, 181
Fitzgerald M. P., Moffat A. F. J., 1974, PASP, 86, 480
Girardi L., Bertelli G., Bressan A., Chiosi C., Groenewegen M. A. T., Marigo P., Salasnich, 2002, A&A, 391, 195
Kharchenko N. V., Piskunov A. E., Röser S., Schilbach E., Scholz R.-D., 2005, A&A, 438, 1163
Landolt A., 1992, AJ, 104, 340
Lejeune T., Schaerer D., 2001, A&A, 366, 538
Lindoff U., Johansson K., 1968, Ark. Astron., 5, 45 (LJ68)
Loktin A., Matkin N. V., 1994, Astron. Astrophys. Trans., 4, 153
Loktin A., Gerasimenko T., Malisheva L., 2001, Astron. Astrophys. Trans., 20, 605 (LGM01)
Lyngå G., 1987, Catalogue of Open Cluster Data. Centre de Donnees Stellaires, Strasbourg
McSwain M. V., Gies D. R., 2005, ApJS, 161, 118
Mermilliod J.-C., Paunzen E., 2003, A&A, 410, 511
Mermilliod J.-C., Andersen J., Mayor M., 1997, A&A, 319, 481
Mermilliod J.-C., Clariá J. J., Andersen J., Piatti A. E., Mayor M., 2001, A&A, 375, 30
Netopil M., Paunzen E., Maitzen H. M., Pinado O. I., Claret A., Miranda L. F., Iliev I. Kh., Casanova V., 2007, A&A, 462, 591
Ng Y. K., Bertelli G., Chiosi C., Bressan A., 1996, A&A, 310, 771
Nilakshi S. R., Pandey A. K., Mohan V., 2002, A&A, 383, 153
Paunzen E., Maitzen H. M., 2001, A&A, 373, 153
Pedreros M. H., 2000, Rev. Mex. Astron. Astrofis., 36, 13
Perryman M. A. C. et al., 1998, A&A, 331, 81
Piatti A. E., Clariá J. J., Minniti D., 1993, JA&A, 14, 145
Piatti A. E., Clariá J. J., Ahumada A. V., 2003a, MNRAS, 340, 1249

Piatti, A. E., Clariá, J. J., Ahumada, A. V., 2003b, MNRAS, 346, 390
Piatti A. E., Clariá J. J., Ahumada A. V., 2004a, MNRAS, 349, 641
Piatti A. E., Clariá J. J., Ahumada A. V., 2004b, A&A, 418, 979
Piatti A. E., Clariá J. J., Ahumada A. V., 2004c, A&A, 421, 991
Piatti A. E., Clariá J. J., Ahumada A. V., 2005, PASP, 117, 22
Piatti A. E., Clariá J. J., Ahumada A. V., 2006a, New Astron., 11, 262
Piatti A. E., Clariá J. J., Ahumada A. V., 2006b, MNRAS, 367, 599
Ramsay G., Pollaco D. L., 1992, A&AS, 94, 73 (RP92)
Ruprecht J., 1966, Bull. Astron. Inst. Czech., 17, 33
Stetson P. B., Davis L. E., Crabtree D. R., 1990, in ASP Conf. Ser. Vol. 8, CCDs in Astronomy. Astron. Soc. Pac., San Francisco, p. 289
Straiys V., 1992, Multicolor Stellar Photometry. Pachart Publishing House, Tucson, AZ
Trumpler R. J., 1930, Lick Obs. Bull., 14, 154
Twarog B. A., Ashman K. M., Anthony-Twarog B. J., 1997, AJ, 114, 2556
Udry S., Mayor M., Queloz D., 1999, in Hearnshaw J. B., Scarfe C. D., eds, ASP Conf. Ser. Vol. 185, Precise Stellar Radial Velocities (IAU Colloq. 170). Astron. Soc. Pac., San Francisco, p. 367
Vandenberg D. A., 1985, ApJS, 58, 711
van den Bergh S., Hagen G. L., 1975, AJ, 80, 11

SUPPLEMENTARY MATERIAL

The following supplementary material is available for this article:

Table 1. CCD *BVI* data of stars in the field of NGC 2489.

This material is available as part of the online article from: http://www.blackwell-synergy.com/doi/abs/10.1111/j.1365-2966.2007.11742.x (this link will take you to the article abstract).

Please note: Blackwell Publishing are not responsible for the content or functionality of any supplementary materials supplied by the authors. Any queries (other than missing material) should be directed to the corresponding author for the article.

This paper has been typeset from a TEX/LATEX file prepared by the author.